Paper No. 61

A GCM SIMULATION OF THE EARTH-ATMOSPHERE RADIATION BALANCE FOR WINTER AND SUMMER

M. L. C. Wu, *National Research Council, Washington, DC and Goddard Space Flight Center, Greenbelt, Maryland*

ABSTRACT

The radiation balance of the earth-atmosphere system simulated by using the general circulation model (GCM) of the Laboratory for Atmospheric Sciences (GLAS) is examined in regards to its geographical distribution, zonally-averaged distribution, and global mean. Most of the main features of the radiation balance at the top of the atmosphere are reasonably simulated, with some differences in the detailed structure of the patterns and intensities for both summer and winter in comparison with values as derived from Nimbus and NOAA (National Oceanic and Atmospheric Administration) satellite observations. Both the capability and defects of the model are discussed.

INTRODUCTION

The GLAS GCM simulates the general features of climatology reasonably well (Halem et al., 1978). Climatological elements, such as the mass distribution, geopotential height, and oceanic rainfall rates generally are in reasonable agreement with observations. Here, we examine the primary driving force, radiation balance, of the circulation system. The GLAS GCM has the feature that the important thermodynamic variables, such as cloud types and cloud heights, atmospheric and ground temperatures, and specific humidity, are interactive with model dynamics, which allows this study to be meaningful. Through a complicated interactive process, in order for the simulated radiation balance at the top of the atmosphere to be right, the kinematics, dynamics, and thermodynamics of the model have to be right. The geographical distribution of the earth-atmosphere system radiation balance from satellite measurements provides a valuable check on our diagnostic studies of the circulation system of the GLAS GCM.

The winter (summer) simulations, starting from real data for 1 January 1975 (15 May 1974), were integrated for 60 days (105 days), and the last 30-day mean was used for comparison with geographical distribution of the radiation balance as derived from Nimbus 3 measurements, for the 14-day (16-day)

mean, starting from 21 January 1970 (16 July 1969). The
zonal mean of the radiation balance was compared with both
Nimbus 3 and NOAA SR measurements (January 1975).

It should be noted that the periods used for comparison
are different since Nimbus 3 data was not available for the
exact period of years for which the model had equilibrated.
It should also be noted that the satellite measurement instru-
ment is not calibrated on board for shortwave measurement;
and it is a sun-synchronous orbit.

The Geographical Distribution of the Radiation Balance of the Earth-Atmosphere System

Global patterns of the radiation balance and its asso-
ciated components, absorbed solar radiation, and outgoing long-
wave radiation, are shown for winter in Figs. 1, 2, and 3,
respectively. Similar distributions for summer are shown in
Figs. 4, 5, and 6. For comparison, values as derived from
Nimbus 3 measurement are displayed in Figs. 1a-6a, and values
as simulated from the model are displayed in Figs. 1b-6b.

Overall, there is reasonably good agreement between the
simulated and the observed radiation balance patterns, particu-
larly for the major energy gain areas over the subtropical mini-
mum cloudiness regions in both summer hemisphere oceans, for
local minima over the continents in summer hemispheres, and for
the zonal pattern of deficit in the winter hemispheres. For
all of these features there is general agreement in patterns,
which indicates that the GLAS GCM is capable of simulating the
general climatology to the accuracy of the zeroth order. The
differences are in the intensities and in the detailed struc-
ture of the patterns. It is from these differences that we
are able to diagnose some of the model defects.

In winter, the simulated zero-balance isoline is around
30N without a southward dip off the west coast of North America,
probably because the model does not generate low stratus clouds,
and with a relatively small southward shift of the zero-balance
isoline over North Africa, probably because the model generates
slightly more cloudiness over Africa especially on the equator-
ward side of North Africa. The simulated period is February,
whereas the observed period is the last two weeks of January.
Due to the sun's declination, there should be about 5° northward
shift of the zero-balance isoline. The cause of the remaining
latitudinal difference may be due to the following reasons.
Generally speaking, the model overestimates total absorbed solar
radiation in the winter hemisphere in comparison with observation
(Fig. 2). In addition, the model systematically underestimates
outgoing longwave radiation (Fig. 3). For example, around 20N,
the simulated value is about .36 cal/cm^2/min, whereas the value
as derived from observation is about .42 cal/cm2/min.

RADIATION BALANCE (cal/cm²/min)

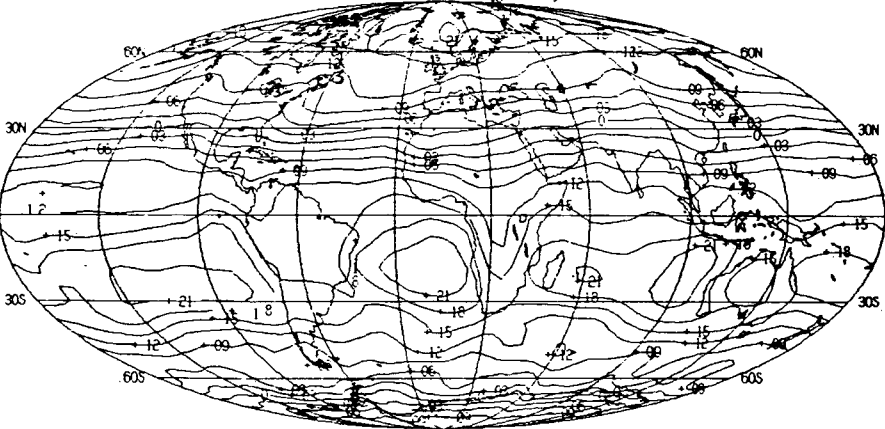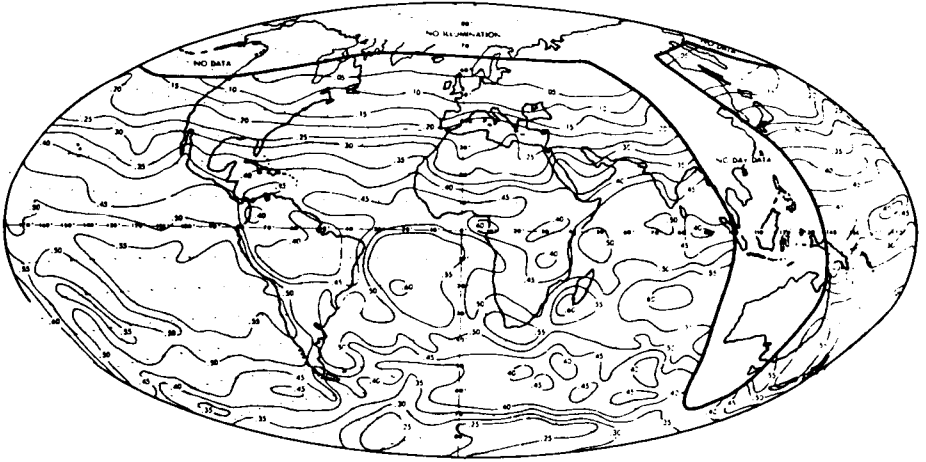### a. Observed (Jan.)

b. Simulated (Feb.)

Fig. 1. Net radiation balance of the earth-atmosphere system

    a.   as derived from Nimbus 3 observations during the period 21 January to 3 February 1970.

    b.   as simulated from the GLAS GCM for February.

369

TOTAL ABSORBED SOLAR RADIATION (cal/cm²/min)

a. Observed (Jan.)

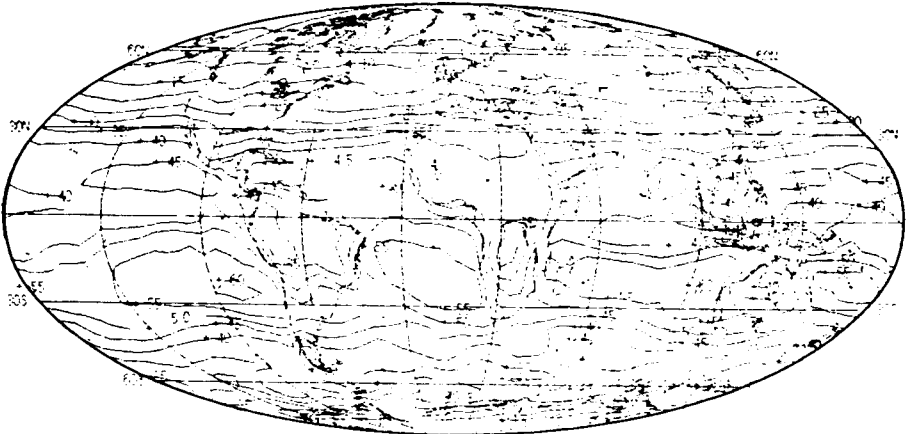b. Simulated (Feb.)

Fig. 2. Total absorbed solar radiation in the earth-atmosphere
system

    a. as derived from Nimbus 3 measurements during the
       period 21 January to 3 February 1970.

    b. as simualted from the GLAS GCM for February.

OUTGOING LONG WAVE RADIATION (cal/cm²/min)

a. Observed (Jan.)

b. Simulated (Feb.)

Fig. 3. Outgoing longwave radiation emitted from the earth-atmo-
sphere system to space

a. as derived from Nimbus 3 measurements during the
period 21 January to 3 February 1970.

b. as simulated from the GLAS GCM for February.

371

RADIATION BALANCE (cal/cm²/min)

a. Observed (July)
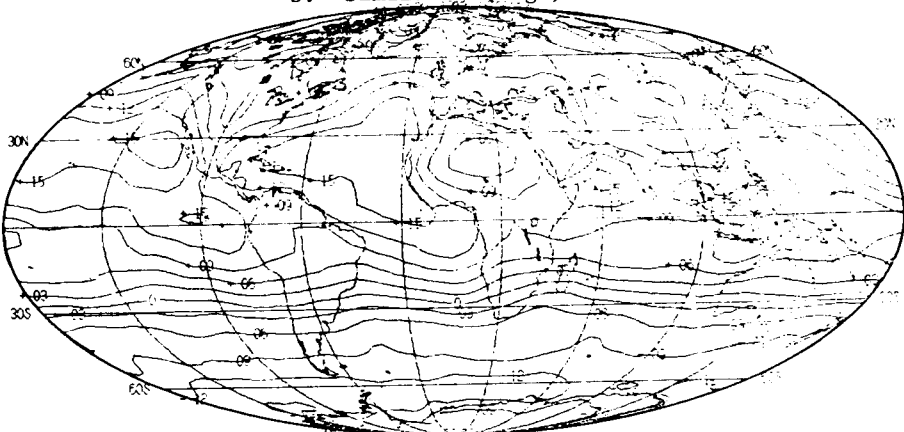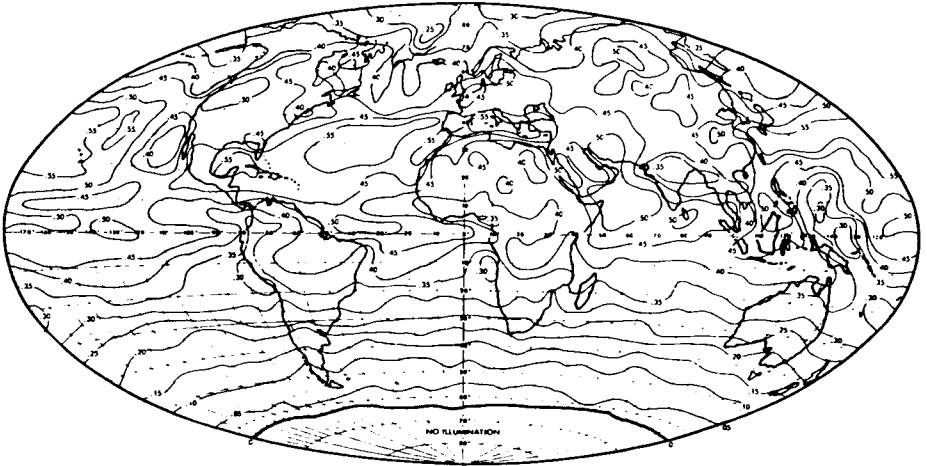

b. Simulated (Aug.)

Fig. 4. Net radiation balance of the earth-atmosphere system

a. as derived from Nimbus 3 measurements during the period 16 to 31 July 1969.

b. as simulated from the GLAS GCM for August.

TOTAL ABSORBED SOLAR RADIATION (cal/cm²/min)
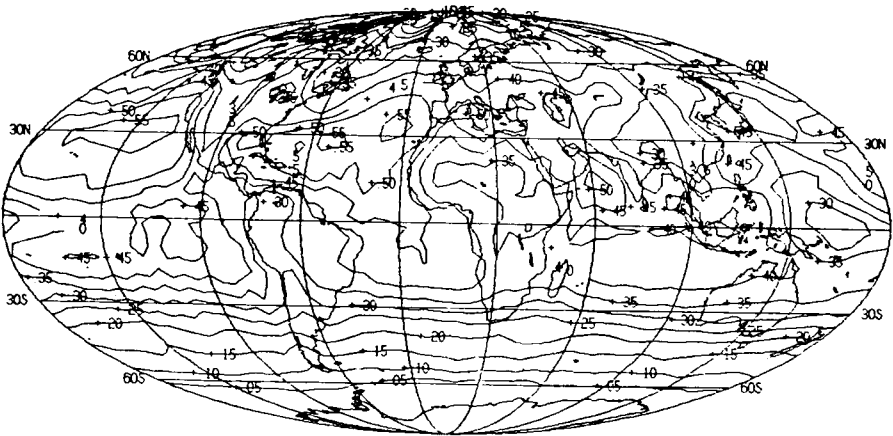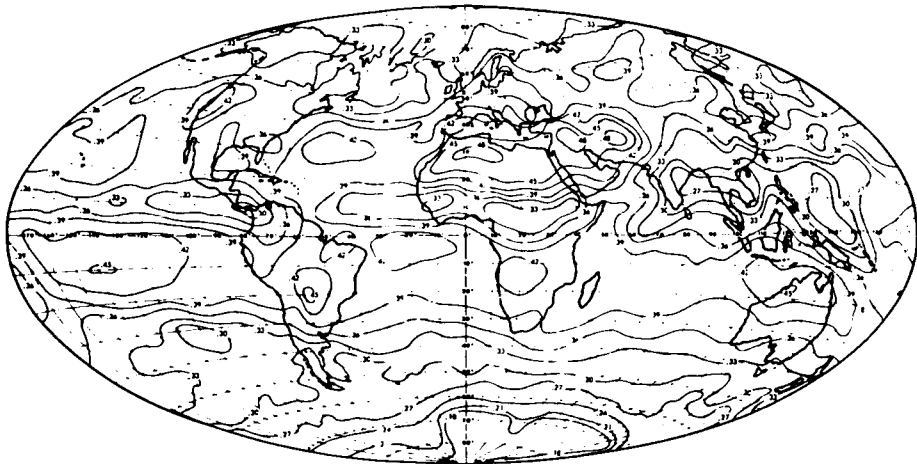
a. Observed (July)

b. Simulated (Aug.)

Fig. 5. Total absorbed solar radiation absorbed in the earth-
atmosphere system

a. as derived from Nimbus 3 measurements during the
period 16 to 21 July 1969.

b. as simulated from the GLAS GCM for August.

OUTGOING LONG WAVE RADIATION (cal/cm²/min)
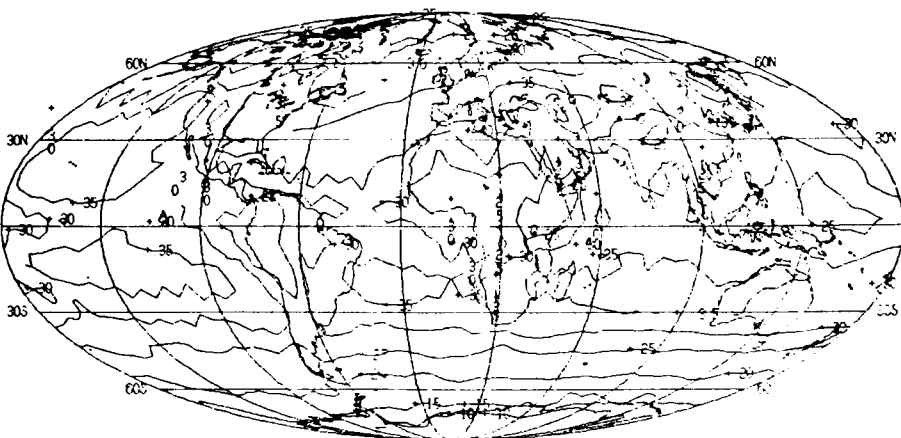
a. Observed (July)

b. Simulated (Aug.)

Fig. 6. Outgoing longwave radiation emitted from the earth–atmo-
sphere system to space

a. as derived from Nimbus 3 measurements during the
period 16 to 21 July 1969.

b. as simulated from the GLAS GCM for August.

374

The major energy gain area is over the Southern Hemisphere with maxima over the oceans in connection with subtropical cloudiness minima, and local minima over continents associated with a heavy ITCZ cloudiness over South America and South Africa around latitude 0 to 20S. The model reproduces maxima over the oceans, because the model simulates subtropical anti-cyclones reasonably well, as well as local minima over the continents.

As would be expected from seasonal change in solar heat-ing, the major energy gain areas are moved to the northern summer for July and August with maximum over the oceans. One striking feature appearing in the summer observations is a deficit in the energy budget over the Sahara and Saudi Arabia. The model produces a more localized minimum over the Sahara, in agreement with the wide-angle radiative balance for August measured with the Earth Radiation Budget (ERB) instrument in Nimbus 6, which also does not show a negative deficit as in the earlier Nimbus 2 and 3 observations. This suggests that part of the discrepancy may be due to the coarseness of resolution of the model. When we examine the separate components of the radiation balance, we find that the deficit is due to high surface albedo and high outgoing longwave radiation. But the particular reason for the deficit to be over the northernmost part of Africa, between 30N and 40N, can be found by examining Figs. 5a and 6a. Fig. 6a is a display of the outgoing longwave radiation. The cloudiness associated with the ITCZ and summer monsoon system are reasonably well revealed in this figure. Fig. 5a shows that the absorbed solar radiation has a more or less uniform distribution with a value of about .4 cal/cm^2/min over North Africa, whereas the outgoing longwave radiation has a strong gradient, starting with a minimum over the equatorward side of north Africa associated with high level clouds over the ITCZ and increasing northward with a maximum on the northernmost part of Africa associated with high surface temperature in a clear area. Thus, a deficit is formed over the northernmost part of Africa. The outgoing longwave radiation in the model does not show a sharp northward gradient over this area and the values over this area are not large enough to produce a deficit. Among the possible reasons are the model-generated cloudiness associated with ITCZ and monsoon system extends too far north and that clouds are assumed to be black emitters and to fill an entire grid area as mentioned above.

More clearly than for winter, some of the differences in the detailed structure of the pattern may be due to the failure of the model to generate low stratus and strato-cumulus clouds over the west coasts of North America, South America, and Africa. For example, instead of a local minimum, the model generates a local maximum over the west coast of North America. The model-generated local maxima with values larger than .12 cal/cm2/min extend too far south and extend into the

Southern Hemisphere over both the eastern Pacific and eastern Atlantic. Moreover, the model-generated cloudiness associated with the ITCZ system over the Atlantic extends too far south. These effects can be seen from Figs. 5b and 6b. Fig. 5b indicates cates that the local maxima with values larger than .45 cal/cm^2/min of the absorbed solar radiation extend too far south into the eastern south Pacific. Fig. 6b indicates that the simulated local maxima outgoing longwave radiation over the south Atlantic is too far south in comparison with observations. The local maxima with values larger than .12 cal/cm^2/min over the Northern Hemisphere also extend too far north (to 40N) over the eastern Pacific and eastern Atlantic, because the model-generated subtropical minimum cloudiness system extends too far north. In other words, cyclonic activities are shifted too far north in the model.

The model does not simulate a deep northwestward dip north of New Guinea, because the cloud systems generated by the model are shifted too far east and have broader structures. The observed zero-balance isoline on the winter hemisphere is around 10S with northward dips over the east and west coasts of both South America and south Africa. The dips over the west coast may be related to the stratus clouds and cloudiness associated with the ITCZ over these regions. The dips over the east coasts may also be related to the clouds over that area. The simulated zero-balance isoline is around 28S. The difference in solar radiation accounts for about an 8° difference in latitudes, but this still leaves a residue difference of about 10°.

As far as the pattern is concerned, the maximum outgoing longwave radiation is confined between 10S and 30S, because the model-generated subtropical minimum cloudiness is located around 10S and 30S. There seems to be a coincidence of the zero-balance isoline with the poleward side of the maximum outgoing longwave radiation for both winter and summer, which appears in both simulated and observed distributions. As for the intensity, we did not take the cloud fraction and cloud transmittance into account in our longwave radiation parameterization, with the result that we tended to underestimate the outgoing longwave radiation.

On the whole, the differences in the detailed structure of the patterns and intensities are either due to: The model failing to generate low-level stratus clouds over the west coasts of North America, South America, and Africa; or differences in detailed structure of the cloud distribution patterns; or the assumption that clouds are black in infrared emission and absorption spectra, and fill an entire grid area. Of course, some of the differences are due to the natural variability of the atmosphere. The above comparison is based on an assumption that values as derived from Nimbus 3 measurement are correct.

Zonally-Averaged Distributions and Global Mean

The zonally-averaged distributions of net heat surplus and deficit with latitude, which are important for the meridional energy transport, are plottted in Fig. 7 for winter comparison. The values as derived from satellite measurement are for January; the values as simulated by model are for February. It should be noted that the observations are taken near 11:30 a.m. (9 a.m.) and 11:30 p.m. (9 p.m.) local standard time for Nimbus 3 (NOAA SR) measurements. Because the model systematically underestimates outgoing longwave radiation, the net radiation balance is overestimated in comparison with results of NOAA SR measurements, but it is overestimated only in the winter hemisphere in comparison with Nimbus 3 measurements.
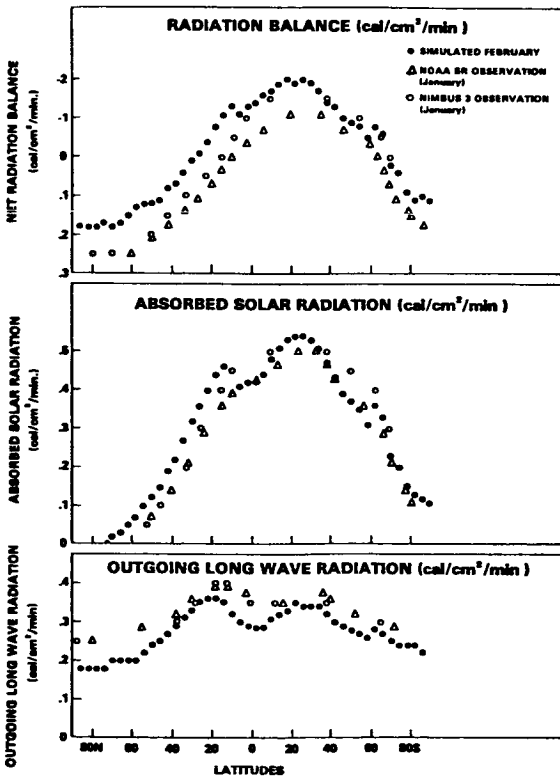

Fig. 7. Zonally-averaged radiation balance.

The global radiation balance is tabulated in Table 1. Because the model-generated longwave radiation is systematically lower than values derived from Nimbus 3 measurements, the model produces a large unbalanced radiation. We have noted above that the overestimated cloud amount and cloud emissivity might account for much of the low outgoing longwave radiation. In addition, the simulated temperature is colder than that of observation; for example, it is almost 10°C to 20°C too cold in polar regions which will also tend to underestimate outgoing longwave radiation.

Table 1. Global radiation budget of the earth-atmosphere system

	Solar radiation cal cm^{-2}min^{-1}			Outgoing Longwave radiation cal cm^{-2}min^{-1}	Radiation balance cal cm^{-2}min^{-1}
	Incoming	Absorbed	Albedo		
Observed (Jan. 21- February 3, 1970)	.501	.361	.283	.337	.024
Simulated (February)	.513	.356	.305	.295	.061
Observed (July 16- July 31, 1969)	.472	.339	.281	.354	-.015
Simulated (August)	.488	.334	.315	.294	.040

Since the sea surface temperature is fixed in the model, we suspect that most of the excess of the unbalanced radiation is lost to the oceans. This can be seen from Table 2, in which the heat balance of the ice-free ocean surface is tabulated. In the model, the sea surface temperature does not change whether the heat balance at the ocean surface is positive or negative. The sensible heat flux, moisture flux, and net long-wave radiation flux in the model depend on the prescibed sea surface temperature. Calculations, results of which are shown in Table 2, indicate that heat loss due to the above fluxes is less than heat gain due to solar flux by .083 cal/cm^2/min (.064 cal/cm^2/min) for February (August) simulations. The global mean, i.e., the above values weighted by fraction of the ice-free ocean (about 66%) is compatible with values of the unbalanced radiation at the top of the atmosphere.

378

Table 2. Heat balance of the ice-free ocean surface
(cal $cm^{-2}min^{-1}$).

	Net solar radiation absorbed by oceans	Net loss through longwave radiation	Loss through sensible heat flux	Loss of heat through evaporation	Net heating of ocean	Global ice-free ocean surface balance
February	.275	.073	.033	.086	.083	.055
August	.168	.042	.018	.044	.064	.042

On an overall basis, the radiation balance of the earth-atmosphere system simulated by using the GLAS GCM is compatible with results as derived from Nimbus 3 observations in geographical distribution of the patterns but with differences in detailed structure of the patterns and in intensities. We think we know some of the causes of these discrepancies and are in the process of trying to eliminate them.

REFERENCES

Gruber, A. 1977: Determinations of the earth-atmosphere radiation budget from NOAA satellite data. NOAA Tech. Rep. NESS 76, Washington, DC.

Halem, M., J. Shukla, Y. Mintz, M. L. Wu, R. Godbole, G. Herman, and Y. Sud, 1978: Comparison of observed seasonal climate features with a winter and summer numerical simulation produced with the GLAS general circulation model. Proceedings of the JOC Study Conf. on Climate Models, April 1978, Washington, DC.

Miller, D. B., 1971: Global atlas of relative cloud cover, 1967-70, U. S. Dept. of Commerce and U. S. Air Force, Washington, D C.

Raschke, E., T. H. Von der Haar, M. Pasternik, and W. R. Bandeen, 1973: The radiation balance of the earth-atmosphere system from Nimbus-3 radiation measurements. NASA TN D-7249, NASA, Washington, DC.

_____, and W. R. Bandeen, 1970: The radiation balance of the planet earth from radiation measurements of the satellite Nimbus II. J. Appl. Meteor., 9, 215-238.

Sadler, J. C., 1968: Average cloudiness in the tropics from satellite observations. East-West Center Press, Honolulu.

Winston, J. S., 1977: Global distribution of cloudiness and radiation as measured from weather satellites. World Survey of Climatology, 6, 247-280.